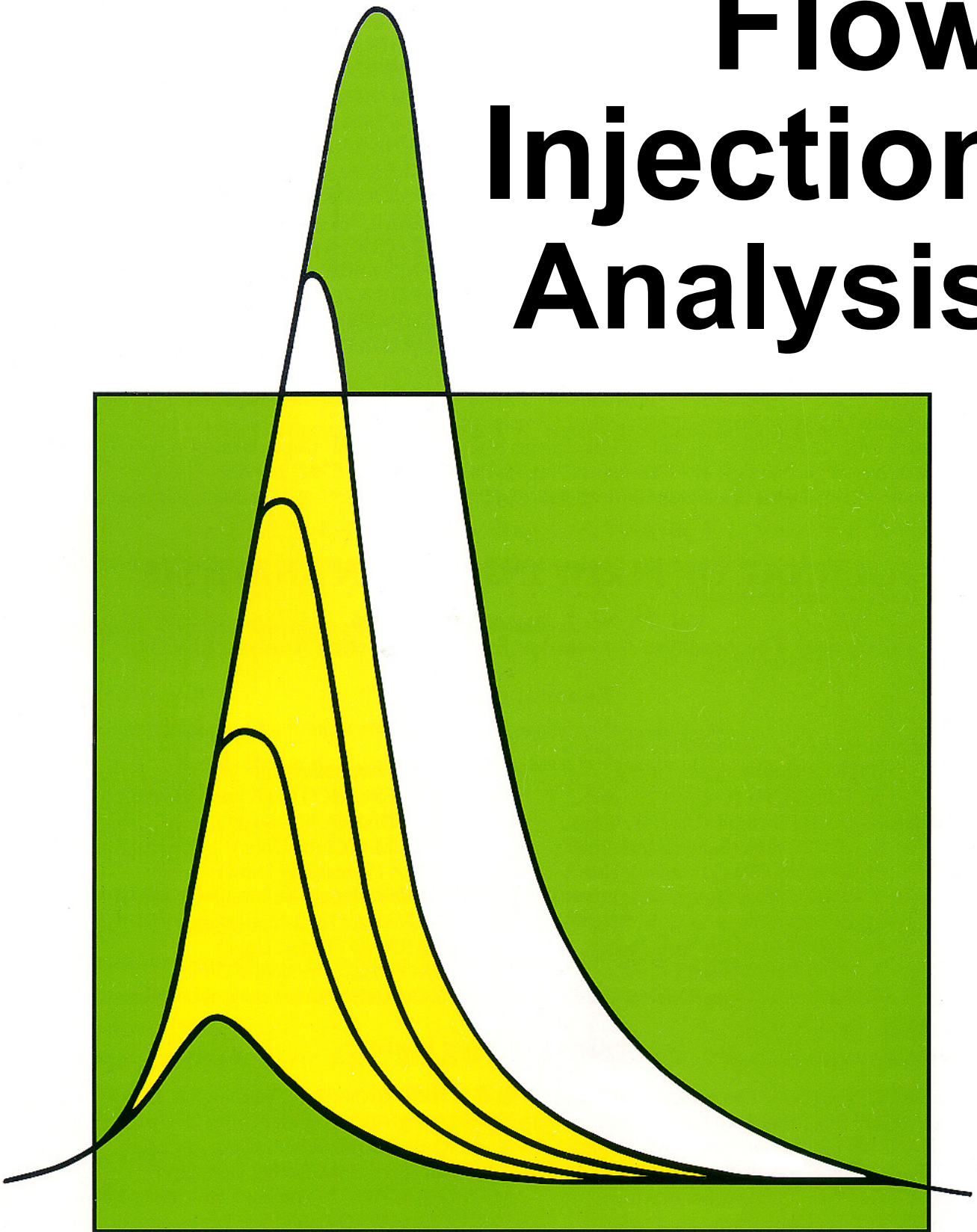


ISSN 0911-775X CODEN: JFIAEA

# JOURNAL OF Flow Injection Analysis



FIA 研究懇談会会誌

# Use of Navier-Stokes and Diffusion-convection Equations in Modeling of Flow-injection Systems

Tomasz Sokalski<sup>1,\*</sup>, Markus Kass<sup>2</sup>, Christian Mueller<sup>3</sup>, Ari Ivaska<sup>1,\*</sup>

<sup>1</sup>Process Chemistry Centre, c/o Laboratory of Analytical Chemistry, Åbo Akademi University, Biskopsgatan 8, FIN-20500 Åbo/Turku, Finland

<sup>2</sup>KWH Mirka, Pensalavägen 210, 66850 Jeppo, Finland

<sup>3</sup>Clyde Bergemann GmbH, Schillwiese 20, D-46485 Wesel, Germany

## Abstract

In this work, mathematical modelling of flow injection analysis is presented. The flow injection analysis (FIA) and sequential flow injection analysis (SIA) manifolds are studied. The mathematical model comprises a system of partial differential equations: i) the Navier-Stokes equation for incompressible fluid flow and ii) the diffusion-convection equation. This system is solved numerically and the resulting profiles of fluid velocity and the concentrations of the species of interest in space and time are obtained. This in turn enables us to obtain signal vs. time curves.

The influence of different parameters, such as fluid velocity, diffusion coefficients and the geometry of the system, on the shape of the signal vs. time curves is analyzed.

The numerical simulation results are compared with the experimental data.

## Keywords

Mathematical modelling, Flow Injection Analysis, Sequential Injection Analysis

## 1. Introduction

Flow injection analysis (FIA) is a versatile technique for manipulation of the solution/sample/reagent followed by different detection methods. It was introduced in the current form in mid 1970s by Ruzicka and Hansen [1] and has since then become a well established analytical method, used in many fields: water analysis, biotechnology, process analysis, life science etc.

It offers high degree of automation and reproducibility at a relatively low cost, while its sensitivity, selectivity and detection limit depend mainly, if not entirely, on the kind of detection method used.

FIA systems can also be miniaturized, which offers various advantages, e.g. portability, reduction of the amount of sample and reagents used and increased speed of analysis.

Use of modelling tools is helpful in developing general design rules and speeds up the development of flow injection systems. However, the first step before using a mathematical design tool is to validate the numerical approach with suitable experimental data from an existing FIA system. In this way, the numerical results obtained for a simulated system can help to optimize new FIA systems.

According to Kolev's excellent and extensive review [2], mathematical models of flow injection (FI) manifolds fall into two main classes: "black box" and analytical-experimental models. Examples of "black box" models are regression equations, neural networks, impulse response functions, and statistical moments. The two main categories of analytical-experimental methods are the probabilistic (random walk) and deterministic models. The deterministic models fall into several categories, such as lumped parameter and distributed parameter methods. The model used in this work belongs to the distributed parameter models and is more specifically a uniform dispersion model.

E-mail: ari.ivaska@abo.fi, tomasz.sokalski@abo.fi

## 2. Theoretical

### 2.1 Physicochemical model

The schematic presentation of the model is shown in Figure 1. The fluid carrier of density  $\rho$  flows with the velocity  $\mathbf{v}$  through a straight tube of the radius  $R$ .



Figure 1. Schematic representation of the used model.

At the time  $t = 0$ , the sample of volume  $V_v$  is injected into the carrier stream. In the case of FI, the flow direction is constant (to the right). In the case of sequential injection (SI), the initial flow direction is to the left. After a certain time the flow is reversed to the right.

### 2.2 Mathematical model

The dynamic behaviour of the fluid is modelled using the Navier-Stokes' equations for incompressible fluid:

$$\rho \left( \frac{\partial \mathbf{v}}{\partial t} + \mathbf{v} \cdot \nabla \mathbf{v} \right) = -\nabla p + \mu \nabla^2 \mathbf{v} + \rho \mathbf{b} \quad (1)$$

$$\nabla \cdot \mathbf{v} = 0 \quad (2)$$

and the equation for the transport of chemical species by diffusion and convection:

$$\frac{\partial c}{\partial t} + \nabla \cdot (D \nabla c + c \cdot \mathbf{v}) = 0 \quad (3)$$

\*Corresponding author

where  $t$  is time [s],  $\rho$  fluid density [ $\text{kg}\cdot\text{m}^{-3}$ ],  $p$  pressure [Pa],  $\mu$  dynamic viscosity [ $\text{kg}\cdot\text{m}^{-1}\cdot\text{s}^{-1}$ ],  $\mathbf{v}$  velocity vector [ $\text{m}\cdot\text{s}^{-1}$ ],  $c$  concentration [ $\text{mol}\cdot\text{m}^{-3}$ ],  $D$  diffusion coefficient [ $\text{m}^2\cdot\text{s}^{-1}$ ].

Because  $v$ ,  $p$  and  $c$  are functions of both space and time, eqs. (1-3) form a system of nonlinear partial differential equations. Such a system cannot be solved analytically for a general case. Therefore, numerical methods have to be used.

### 1.3 Numerical implementation

Two commercially available programs were used to solve the problem.

#### 1.3.1. Femlab

Femlab v. 2.3 (Comsol AB) is an interactive environment for modelling and solving scientific and engineering problems based on partial differential equations using the finite element method (FEM).

Because of the big differences in radial and axial dimensions ( $r = 0.76$  mm and  $L = 4$  m), the problem is scaled down 100 times in the axial dimension. The resulting domain has the dimensions 0.00076 m in the Y direction and 0.04 m in the X direction. The applied mesh consists of 9984 elements.

#### 1.3.2. Fluent

Fluent (ANSYS, Inc.) is a general-purpose CFD code based on the finite volume method.

Computational Fluid Dynamic simulations are performed on computational meshes consisting of a number of connected computational cells, representing the physical volume to be studied (Fig. 2). The total number of cells in the mesh used in this study was around 90.000. The mesh is highly resolved along the tube wall to be able to consider possible wall effects. The sample section and the part of the mixing section behind the detector plane are meshed with a higher resolution.

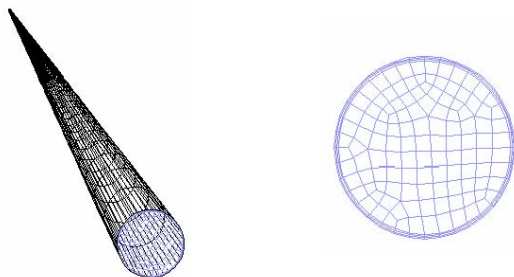


**Figure 2. Left:** Computational mesh representing the physical dimensions of the Flow Injection Analysis (FIA) system studied **Right:** Cross section through the computational mesh in the inflow section

Each simulation consists of two parts: i) a steady state calculation of the carrier flowing through the tube and ii) a time-dependent calculation of the sample flowing and dispersing in the carrier together with a recording of the response curve at the detector plane.

### 1.4. Construction of a tracer curve

The example tracer curve was constructed using  $D = 10^{-8} \text{ m}^2 \text{ s}^{-1}$ , and flow rate 50  $\mu\text{L/s}$ .

#### 1.4.1. Velocity of the fluid

In order to construct a tracer curve the velocity of the fluid was first calculated using the Navier-Stokes equation (Eqs. 1-2). Fig. 3 shows the example velocity profile of the fluid in the tube and the cross section of the tube at a given distance from the point of

sample injection. As can be seen in Fig. 3, even after a very short time (0.5 seconds) the flow velocity already has a fully developed parabolic profile.

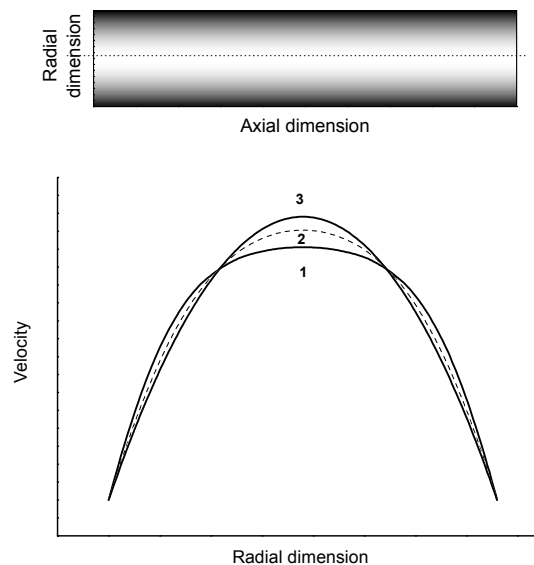


**Figure 3. Top:** Carrier velocity surface plot at 0.5 s; the darker the colour, the slower the velocity. **Bottom:** Cross section plot at 0.5 m from the injection point and at 0.01 (1), 0.02 (2) and 0.5 (3) seconds.

#### 1.4.2. Concentration profiles

After calculating the velocity profiles, we can insert them into the diffusion-convection equation to obtain the concentration profiles at any given time and in any place in the space. This is illustrated in Fig.4, where the dispersion of the injected sample is shown at selected time after injection.

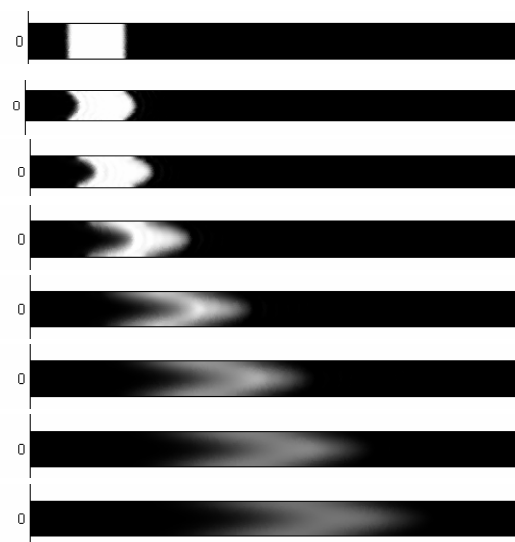


**Figure 4.** Concentration profiles of an injected sample plug at (from top to bottom) 0, 0.4, 0.8, 2, 4, 6, 8, 10 s.

The corresponding cross section plot of the concentration profile of the sample plug at a fixed distance (e.g. in the detector) from the injection point is shown in Fig. 5. We can see in Fig. 5 (top) that as the time progresses, the concentration “seen” by the detector increases and reaches a maximum value.

As the tail of the sample plug passes the observation point (the detector), the concentration gradually decreases and the curves of the cross section plot change accordingly (bottom).

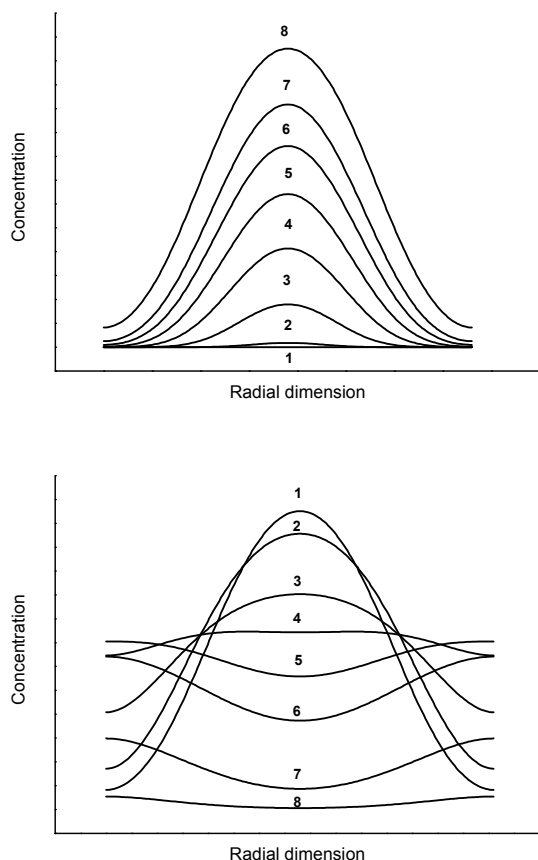


**Figure 5.** Concentration profiles at different times at a fixed distance (e.g. in the detector) from the injection point. **Top:** Increasing concentration. Curves 1–8 were obtained at 5.0, 5.1, 5.2, 5.3, 5.4, 5.5, 5.6, 5.8 seconds after sample injection. **Bottom:** Decreasing concentration. Curves 1-8 were obtained at 5.8, 6.0, 6.5, 7.5, 8.5, 9.5, 12.0 and 15.0 seconds after sample injection. The figure was divided into two parts for the sake of clarity.

### 2.3. Tracer Curves

Since in the experimental part the spectrophotometric detection method is used, the simulation procedure must also reflect this fact. According to Lambert-Beer's law, the absorbance is linearly dependent on the concentration of the determined substance. But because the concentration profile along the radial dimension is not constant, we have to integrate the absorbance over the light path.

$$A = \varepsilon \cdot \int_0^d c(y) dy \approx \varepsilon \cdot \sum_{y_i=1}^N c_{y_i} \cdot \Delta y \quad (4)$$

where  $A$  is the absorbance,  $\varepsilon$  is the molar extinction coefficient, and  $c(y)$  is the concentration of the determined substance in the radial direction. The tracer curve is shown in Fig. 6.

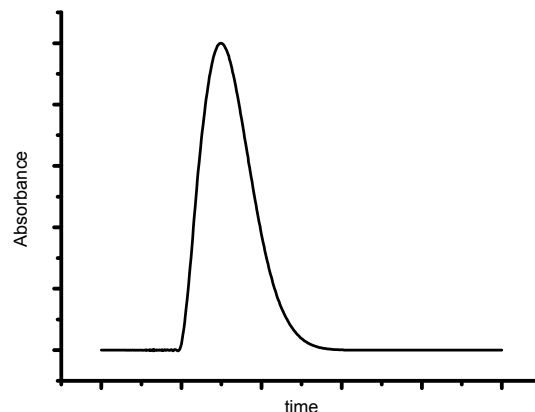


**Figure 6.** Tracer curve obtained using  $D=10^{-8} \text{ m}^2 \text{ s}^{-1}$ , and flow rate  $50 \mu\text{L/s}$ .

## 3. Experimental

### 3.1. Chemicals

A solution of bromothymol blue (BTB) was prepared by adding 0.4 g of BTB to 25 ml 96% ethanol and diluting the solution to 100 ml with 0.01 M sodium tetraborate. The solution was diluted further, making the final BTB concentration 0.016 g/l, and was used in the experiments where tracer curves were recorded. Distilled and deionized water was used for dilution and as the carrier solution in the SIA and FIA systems throughout the experiments.

### 3.2. Equipment

The SIA experiments were performed using a sequential injection flow system, SIAMate™ analyser from Arctic Instruments Oy Ab (Turku, Finland) [3] shown in Fig. 7. The instrument has a zoomable LED based photometer with a 0.76 mm light path. The absorbance was measured at 635 nm in the tracer experiments. The AnalySIA software was used to control the experimental parameters.

The volume of the SIA syringe pump was 2.5 ml and the volume of the sample loop was 65  $\mu\text{l}$ . The length of the tubing going from the sample loop to the detector was 25, 50 and 100 cm. The flow rate was varied between 25, 33, 40 and 50  $\mu\text{l/s}$ . All tubing used in the system was made of polytetrafluoroethylene and had an inner diameter of 0.76 mm.

FIA experiments were carried out using FIALab-2000, a manually operated solution handling system with a four channel peristaltic pump and a two-position six-port injection valve. Because the timing and reproducibility of our FIA system was too poor to be used in these applications, FIALab-2000 was connected to the SIA system as shown in Figure 8. With this setup we were also able to use the more accurate SIA detector.

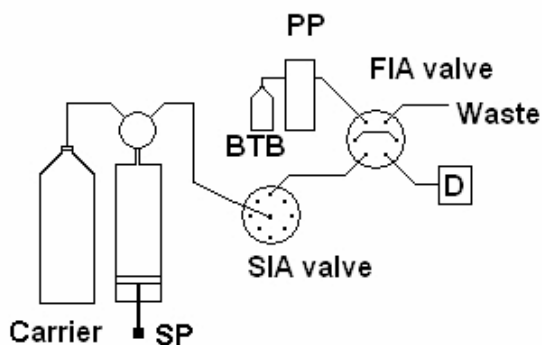


**Figure 7.** Schematic picture of the flow injection system used in the experiments. SP is the SIA syringe pump, PP the FIA peristaltic pump and D is the detector.

### 3.3. Procedure

The tracer measurements were performed according to the following procedure: (1) The FIA pump was started and the sample loop was filled with the BTB solution. (2) The FIA pump was stopped. (3) The FIA valve was turned to load position. (4) The SIA measurement cycle was started. (5) The SIA syringe was filled with carrier solution. (6) The SIA valve was turned to detector position. (7) While emptying the SIA syringe, the absorbance was recorded in the detector unit.

Steps 1-4 were done manually and steps 5-7 were automatic. The median values of at least three repetitions were used for each experiment.

## 4. Results and discussion

The most important causes of radial dispersion in flow-injection systems are molecular diffusion, turbulent flow and secondary flow. The extent of radial mixing primarily depends on whether the flow is laminar or turbulent. At low values (less than 2100) of Reynolds number,  $Re = 2Rv\rho/\mu$ , the flow is usually assumed to be laminar.

Because the dimensions and flow rates used in FI ( $Re < 130$ ), all the cases of FI considered here (provided that the tube is not coiled) should fall very easily within the range of laminar flow and, consequently, the radial dispersion should be governed by diffusion alone.

Fig. 8 illustrates the influence of (the magnitude of) the diffusion coefficient on the shape of the tracer (FIA) curve.

The reduced time is defined as  $\tau = D \cdot t / R^2$ . For small values of reduced time the radial transfer is negligible and the sharp rise of the peak followed by an exponential decay is observed. For medium values of  $\tau$  a double-humped peak is observed. For big values of  $\tau$  a nearly Gaussian, slightly skewed peak is observed.

The obtained results correspond well to the literature observations as presented by Vanderslice et al. [4].

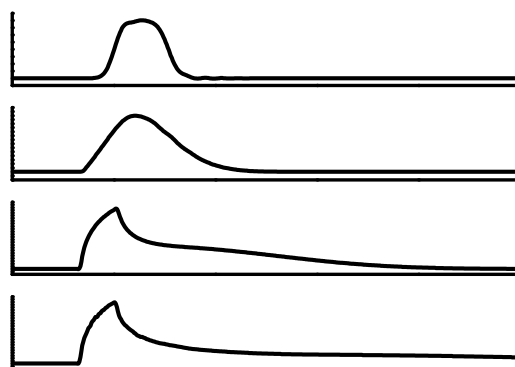


**Figure 8.** Influence of different diffusion coefficient values on the shape of the tracer curve. The value of the diffusion coefficient used was (from top to bottom)  $10^{-7}$ ,  $10^{-8}$ ,  $10^{-9}$ ,  $10^{-10}$   $m^2 s^{-1}$ . The corresponding  $\tau$  values are: 7 0.7, 0.07 0.007 respectively.

In order to examine the applicability of the used model, the following FI systems were simulated: a) micro-flow system b) FIA system c) SIA system.

### 4.1. $\mu$ -FIA

Figure 9 shows the theoretical curves calculated according to our model using the physical parameters of the micro-FIA system described by Van Akker[5,6]. Our results agree well with van Akker's experimental data and theoretical simulations.

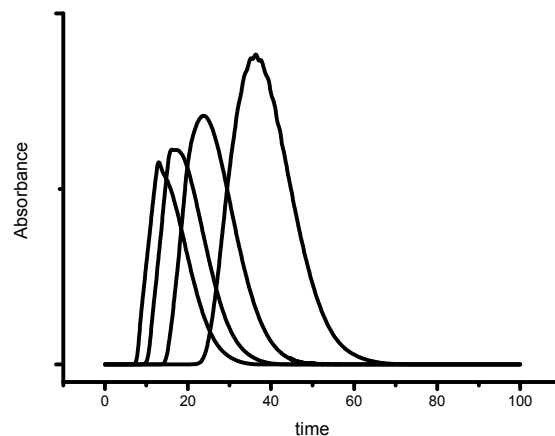


**Figure 9.** Simulated curves for the  $\mu$ -FIA-system described by Van Akker[5,6]. The experimental parameters, i.e. the flow rates (from left to right: 5, 4, 3 and 2  $\mu l/min$ ) and the value of the diffusion coefficient ( $3 \cdot 10^{-10}$   $m^2 s^{-1}$ ) are the same as those used by Van Akker.

### 4.2. FIA and SIA

Figures 10 and 11 show the comparison of theoretical predictions with the results from experiments with different flow rates for the FIA system described in the experimental part.

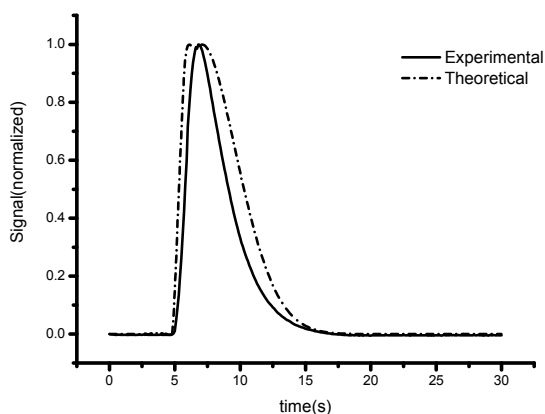


**Figure 10.** Comparison of theoretical and experimental curves for FIA system. The experimental flow rate was 50  $\mu\text{L/s}$ . The diffusion coefficient value used in the simulation was  $10^{-8} \text{ m}^2/\text{s}$ .

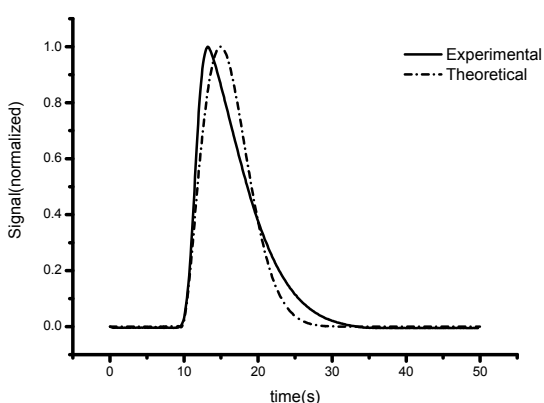


**Figure 11.** Comparison of theoretical and experimental curves for FIA system. The experimental flow rate was 25  $\mu\text{L/s}$ . The diffusion coefficient value used in the simulation was  $10^{-8} \text{ m}^2/\text{s}$ .

The obtained results show good agreement between experimental and theoretical curves. However, the diffusion coefficient for which the best agreement was obtained was of the order of magnitude of  $10^{-8} \text{ m}^2/\text{s}$ . This value is much greater than the experimental values for BTB in water solutions given in the literature which is of the order of magnitude of  $10^{-10} \text{ m}^2/\text{s}$ .

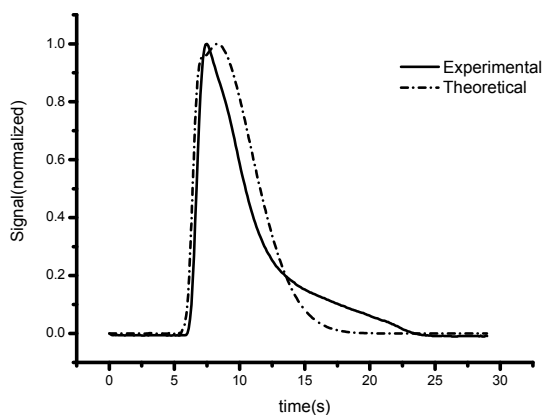


**Figure 12.** Comparison of theoretical and experimental curves for SIA system. The experimental flow rate was 50  $\mu\text{L/s}$ . The diffusion coefficient value used in the simulation was  $10^{-8} \text{ m}^2/\text{s}$ .

Similar results were obtained for the SIA system with the flow rate 50  $\mu\text{L/s}$  (Fig. 11) as well as for FIA and SIA systems for other flow rates (33 and 40  $\mu\text{L/s}$ ).

All the systems investigated in this study had a very low Reynolds number. For FIA with the flow rate  $V=50 \mu\text{L/s}$ ,  $\text{Re} = 84$  and for  $\mu\text{-FIA}$  with  $V= 0.033 \mu\text{L/s}$ ,  $\text{Re} = 0.3$ . Consequently, in both cases the flow should be fully laminar.

However, a comparison between the experimental and theoretical results proves that this is not the case. For the  $\mu\text{-FIA}$  system considered in this work, a physically and experimentally sound value of the diffusion coefficient ( $\sim 10^{-10} \text{ m}^2/\text{s}$ ) can be used.

In contrast, to obtain an adequate agreement for the FIA and SIA systems, a diffusion coefficient value of  $\sim 10^{-8} \text{ m}^2/\text{s}$  must be used, a fact which suggests that in this case, the flow is not completely laminar. Additional factors beside the molecular diffusion obviously contribute to the faster transport in the radial direction.

We propose the use of the term “conditional” diffusion coefficient for a given experimental system to account for the additional radial mixing.

## 5. Conclusions

It is commonly accepted that in most FI systems the flow is entirely laminar and that the diffusion coefficient provides the main contribution to the radial mixing. We examined this claim using the Navier-Stokes and diffusion-convection equations. The theory was checked against the experimental data.

For  $\mu\text{-Fia}$  systems, the physically relevant diffusion coefficient value of ca  $10^{-10} \text{ m}^2/\text{s}$  provided good agreement between theory and experiment. For classical FIA systems, a much higher diffusion coefficient value of ca  $10^{-8} \text{ m}^2/\text{s}$  had to be used.

There are some additional contributions to the radial mixing. Consequently, in this case, the use of the term “conditional diffusion coefficient” is proposed.

## Acknowledgements

This work is a part of MASTRA MATERA ERA-NET project funded under the 6<sup>th</sup> FP EU.

This work is part of the activities of the Åbo Akademi Process Chemistry Centre within the Finnish Centre of Excellence programme (2000-2011) supported by the Academy of Finland

## References

1. J.Ruzicka, E.H.Hansen; *Analytica Chimica Acta* **1975**, *78*, 145-157.
2. S.D.Kolev; *Analytica Chimica Acta* **1995**, *308*, 36-66.
3. N.Kullberg, M.Vilen, P.Sund, M.Talasilahti, R.Sara; *Talanta* **1999**, *49*, 961-968.
4. J.T.Vanderslice, A.G.Rosenfeld, G.R.Beecher; *Analytica Chimica Acta* **1986**, *179*, 119-129.
5. E.B.van Akker, M.Bos, W.E.van der Linden; *Analytica Chimica Acta* **1999**, *378*, 111-117.
6. E. B. van Akker; PhD *Thesis*, **1999**, University of Twente, Enschede, The Netherlands.

(Received May 13, 2008)  
(Accepted June 1, 2008)